Sarraf H, et al., J Nanotechnol Nanomed Nanobiotechnol 2016, 3: 010
DOI: 10.24966/NTMB-2044/100010

HSOA Journal of
Nanotechnology: Nanomedicine & Nanobiotechnology

Research Article

Evaluation of the Effect of Solid Loadings on Rheological Properties of Highly Concentrated Biocompatible Nanoparticle Suspensions

H Sarraf[1, 2, 3, 4]*, L Skarpova[3], J Havrda[3], L Bartovska[3], M Maryska[3], V Hulínsky[3], H Akbari[5] and A Sadr[6]

[1]*Nanoprodex LLC, NW, 48th Ave, Vancouver, WA 98685, USA*

[2]*Western Governors University, 1001 Fourth Avenue, Seattle, WA 98154-1101, USA*

[3]*University of Chemical Technology, Technicka 5, 166 28, Prague 6, Czech Republic*

[4]*Department of Metallurgy and Ceramics Science, Tokyo Institute of Technology, 2-12-1 Ookayama, Meguro-ku, Tokyo 152-8550, Japan*

[5]*University of Pennsylvania, 3600 Market Street, Suite 380, Philadelphia PA 19104, USA*

[6]*University of Washington, School of Dentistry, Seattle, WA 98195-7456, USA*

Abstract

Preparation and colloidal dispersion of highly concentrated biocompatible nanoparticles suspensions are vital for fabrication of dense bioceramic nanocomposites with improved mechanical and microstructural properties for biomedicine applications. This paper presents formation and rheological characterization of highly concentrated biocompatible aqueous ZrO_2 nanosuspensions for such applications. The rheological properties including viscosity (η), shear rate (γ), and shear stress (τ) were investigated in relation to a wide range of solid loading (ϕ, by weight = 75 - 78 mass%). Maximum solid loading (ϕ_{max}) was estimated with a constant 0.9 mass% concentration of a new type of anionic polyelectrolyte Dolapix CE64, suitable for casting of materials. A colloidal model was proposed to visualize the effect of solid loading on colloidal stability, rheological behavior and green microstructure of samples after casting. The maximum solid loading (ϕ_{max}) was estimated to be 77 mass% based on the dependence of both viscosity (η) and yield stress (τ_0) on solid loading (ϕ). For further validation, the maximum solid loading was compared and fittedby different rheological flow models with a correlation factor r = 0.998 for Herschel-Bulkley model, r = 0.999 forPower law model and r = 0.920 for Bingham model at shear rate γ (50 s^{-1}). All concentrated ZrO_2 nanosuspensions exhibited shear-thinning behaviour. The results obtained from rheological measurements, scanning electron microscopy imaging and flow models validate our proposed hypothesis for prediction of maximum solid loading and visualization of quality of green microstructures after casting. These results contribute to preparation, characterization, and processing of highly concentrated bio/nanoparticles suspensions; aiming to fabricate highly dense bio/nanocomposite materials with specific functionality.

Keywords: Anionic polyelectrolyte dispersant Dolapix CE64; Flow models; Rheology; Viscosity; Yield stress; ZrO_2 nanoparticle

Abbreviations

Dolapix CE64: A commercial name of an anionic polyelectrolyte dispersant
HR-TEM: High Resolution- Transmission Electron Microscope
SEM: Scanning Electron Microscope
(ϕ): Solid loading
(ϕ_{max}): Maximum solid loading
γ (1/s): Shear rate
τ (Pa): Shear stress
η (Pa.s): Viscosity
(τ_0): Yield stress

Background

Colloidal processing of bio/nanoparticles and characterization of their rheological properties in different concentrated aqueous suspension shave received an increasing amount of attention, especially for fabrication of dense bio/nano ceramic composites with improved mechanical and microstructural properties for biomedical engineering [1-6]. Zirconia (ZrO_2) based bio/nano ceramics have received a valuable attention in biomedical engineering in recent years [6,7]. ZrO_2-based multiphase nanoparticles have been used to reinforce biological matrices such as collagen, enhancing its mechanical and thermal properties and leading to hybrid materials with potential use in biomedical, bionic, and dental applications such as bridges, crowns, inserts, and implants [8-11].

From a technological point of view, in order to fabricate dense ZrO_2-based bioceramic materials with uniform microstructure and good mechanical properties, it is vital to start with a highly concentrated nanopowder suspension with an appropriate dispersant stabilizer using colloidal processing techniques [12]. However, fabrication of ZrO_2 bio/nano ceramic composites through colloidal processing methods require stable, well-dispersed nanosuspensions with extremely high levels of solid loading to achieve optimal casting condition, green body properties. In addition, colloidal methods can minimize drying-induced shrinkage leading to defect-free microstructure with improved mechanical properties and reliability [13-15]. In all types of colloidal processing techniques, such as tape casting [16], slip casting [1-3], centrifugal casting [17,18], pressure casting [19], freeze casting [20], injection molding [21], dip coating [22] and direct ink writing [23], rheological properties of

***Corresponding author:** H Sarraf, Nanoprodex LLC, NW, 48th Ave, Vancouver, WA 98685, USA, Tel: +1 2068172688; E-mail: info@nanoprodex.com; hsarraf@wgu.edu

Citation: Sarraf H, Skarpova L, Havrda J, Bartovska L, Maryska M, et al. (2016) Evaluation of the Effect of Solid Loadings on Rheological Properties of Highly Concentrated Biocompatible Nanoparticle Suspensions. J Nanotechnol Nanomed Nanobiotechnol 3: 010.

Received: March 07, 2016; **Accepted:** April 20, 2016; **Published:** April 30, 2016

concentrated suspensions with high solids loading play a key role in controlling the shape forming behavior and optimizing the properties of the green and final sintered bodies [24].

Fundamentally, the rheological properties of concentrated colloidal nanoparticles suspensions are determined by interplay of thermodynamic interactions [3]. This means that there exists an intimate relation between the nanoparticle interactions, the suspension structure (i.e., the spatial particle distribution in the liquid), and the rheological response. However, the combination of high solids loading and nanoparticles leads to a viscosity and thixotropy increase because of increased nanoparticle-nanoparticle interactions and, consequently, to difficulties in slurry casting process [3,25,26]. Addition of suitable dispersant not only can dramatically reduce the viscosity and thixotropy of slurries with very high solids loading, but also can lead to fabricating of defect-free, dense and high quality nano-bio products [27,28].

Several studies have revealed that colloidal systems that contain a polyelectrolyte-based dispersant, which is functioning via electrosteric stabilization mechanism, have an especially important role in colloidal processing of nano/bio ceramics [29-31]. Polyelectrolyte-based dispersants exhibit several advantages over inorganic dispersants, including greater stability; greater control of the thixotropy, the possibility to prepare highly concentrated suspensions, with higher consolidated density for casting, and greater flexibility for processing multiphase systems [32-34]. Previously, several researchers examined various water-soluble anionic polyelectrolyte dispersants such as PAA, PMAA, and Darvan for the stabilization of low concentrated oxide powder slurries (alumina, titania, zirconia, etc.) with average particle size of less than 1 μm [34-36]. Recently, we have reported fabrication of a new type of very dense and fine-grained alumina-toughened zirconia (Al_2O_3-ZrO_2) bioceramic composite by optimizing processing parameters with emphasis on improving and controlling fine grain growth, which leads to formation of homogeneous compact desirable microstructures using colloidal processing [36]. High concentrated Al_2O_3-ZrO_2 suspensions were well-dispersed with the help of an optimal amount 0.9 mass% of a new commercial type of electrosteric polyelectrolyte (Dolapix CE64, Zschimmer & Schwartz GmbH Co., Germany), as a suitable dispersant [36]. Accordingly, in this paper we have applied a primary amount of 0.9 mass% Dolapix CE64 for fabrication and dispersion of highly concentrated aqueous ZrO_2 nanoparticles suspensions at different solids loading in the range of 75 mass% to 78 mass%, aiming to gain maximum solids loading suitable for casting applications and fabrication of biocompatible ZrO_2 nanoceramics.

Accordingly, several rheological flow models have been developed for non-Newtonian systems, including the power law model, Bingham plastic model, the Herschel-Bulkley model, and the Casson model [37,38]. These models have been widely and successfully used to explain, characterize, and predict flow and shear-thinning behaviors for various systems. However, the study of shear-thinning behavior of high concentrated ZrO_2 nanosuspensions/Dolapix CE64 systems by means of these models is still limited. And not much work has been reported yet.

Thus, the primary purpose of the present study is to investigate the maximum solids loading of concentrated ZrO_2 nanosuspensions in the presence of a constant concentration of 0.9 mass% dispersant (Dolapix CE64) through rheology study. Consequently, viscosity measurements were carried out to discuss shear-thinning behavior and to correlate the rheological (viscosity, yield stress and shear rate) properties and dispersion effects of anionic polyelectrolyte dispersant by three different rheological flow models of the ZrO_2 nanosuspensions.

We've also intended to demonstrate the effect of solid loadings on stabilization of concentrated ZrO_2 nanosuspensions and related green microstructures that were prepared after slip casting and drying processes by Scanning Electron Microscopy (SEM) analysis.

Finally, we have hypothesized a schematic model to illustrate the role of solids loading and the adsorbed anionic polyelectrolyte distribution on nanoparticle surface. Our proposed hypothesis illustrates the stability of ceramic suspensions in nanometer scale and the packing quality of green microstructures after slip casting and drying processes.

Materials and Methods

ZrO_2 nanopowder

The biocompatible [5,9,39-41] ZrO_2 nanopowder (99.99% purity, Tosoh Corp., Japan) was used in this study which has a bulk density of 6.05 g/cm^3 and surface area (by BET) of (13.0-19.0) 16.0 m^2/g. Morphology of ZrO_2 nanopowder (Figure 1) was observed by a high-resolution transmission electron microscope (FE-TEM, JEOL JEM-2010F,Center for Materials Analysis, Tokyo Institute of Technology).

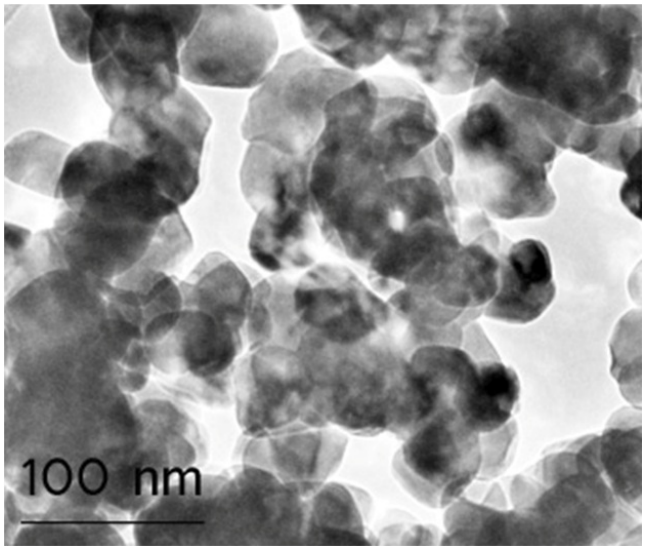

Figure 1: TEM image of aggregated bare ZrO_2 nanoparticles with a primary nanocrystallite size of 40 nm.

Dispersant characterization

Of the different water-soluble anionic polyelectrolyte dispersants available (e.g., PAA, PMAA), a new type of commercially available electrosteric dispersant agent, Dolapix CE64 (Zschimmer & Schwartz GmbH Co., Germany) was found to be the most suitable choice on basis of physical and chemical properties as well as practical experiments reported by different authors [3,42-52]. According to the manufacturer information and result reported by different authors, Dolapix CE64 contains aqueous solution (~ 70 mass%) and ammonium salt (~ 30 mass%) of poly-(methacrylic acid) (PMAA-NH_4) , with a pH of 9 [3,43-52].It has a molecular weight of 660 g/mol with a density (20°C) of approximately 1.2 g/cm^3 [3,43-52]. It can easily dissociate in water and produces negatively

charged polyions and ammonium counter-ions that create stability based on electrosteric interactions [3,43-52]. Therefore, in this study Dolapix CE64 was used for highly concentrated suspensions stabilization.Dispersant concentration and solids concentration are both calculated in percentage by weight (abbreviated mass%) on dry powder basis.

Nanosuspensions preparation

In this study, we aimed (i) to prepare ZrO_2 nanosuspensions with the maximum solids (ϕ_{max}) loading and (ii) to analyze the effect of solid loadings (ϕ) on the rheological properties (e.g., shear rate (γ), shear stress (τ), and viscosity (η)) of prepared suspensions for casting applications.To gain maximum solids loading, fourseries of nanosuspensions were prepared with doubly distilled water by different solid loadings in the range of 75-78 mass% with addition of a constant primary amount 0.9 mass% of dispersant Dolapix CE64.

Resulting suspensions were dispersed by using a planetary ball-mill (Pulverisette 6, Fritsch, Germany) for a period of 30 min at a rate of 500 rad/min. Subsequently, deagglomeration was performed in vacuum (laboratory desiccator, pressure < 50 mbar) to remove gas bubbles for 5 min. Then suspensions were additionally deagglomerated with a high-energy ultrasonic horn (Qsonica, with applied amplitude of up to 60 μm) for 5 min and again degassed for an additional 5 min for removal of air bubbles and better homogeneity, which is essential prior to rheological measurements as well as for slip casting. pH of all nanosuspensions during suspension preparation was determined at equivalent value of 9 [26,36,42]. At least ten suspensions were prepared for each different nanosuspension compositions, in order to determine the maximum solid loading with a constant 0.9 mass% dispersant to give the optimal viscosity and control reproducibility of suspensions.

Rheological characterization of nanosuspensions

Immediately after preparation of four groups of nanosuspensions, selected nanosuspensions were evaluated with respect to their rheology, by means of viscosity measurements. Viscosity measurements were carried out by using a concentric cylindrical rheometer (Thermo Haake Ltd., Sensor Z41-DIN measurement system, RV1, Germany). For rheological characterization of selected nanosuspensions, the following three key points were focused: (i) effect of maximum solid loading on aqueous suspensions in the presence of constant 0.9 mass% dispersant concentration, (ii) application of different flow models, and (iii) estimation of the yield value (τ_0) on the stability of concentrated ZrO_2 nanosuspensions.

The flow curves were automatically recorded via a built-in program at a particular temperature 23 ± 1°C. Experimentally, for measuring of all suspensions a volume of about 14 ml was obtained and used in cylinder. Before performing rheological characterization, to avoid undesired influence from different mechanical histories, the fresh samples were pre-sheared by shearing at an identical rate of 100 s^{-1} for 1 min, followed by an equilibrium period of 2 min prior to measurement. Then, immediately rheology (viscosity) of suspensions was determined. The measurements were performed with the following input conditions: The shear rate (γ) increased (forwards) continuously, and then also reversed (backwards) to 0 s^{-1} with 21 equal steps in the range of shear rates from 0.03 s^{-1} to 1000 s^{-1} over a time period of 20 min. This range was scanned forwards and then backwards in order to check if a given sample was shear-stable or thixotropic [53-55]. Thrice measurements were made for each suspension, and each result was identical on the whole. The influence of solids loading on the viscosity and yield stress (τ_0) of concentrated ZrO_2 suspensions are investigated by using different rheological flow models. The flow curves (shear stress versus shear rate, viscosity versus shear rate) at a particular shear rates between the range of γ < 0.03 s^{-1} - 1000 s^{-1}> are calculated automatically by Rheowin software (Rheometer, Haake Instrument, Germany), compared and corrected by excel software program. The yield stress (τ_0) was calculated directly by Rheowin software program for three rheological flow models of: power law, Bingham plastic, and the Herschel-Bulkley and then compared by shear stress obtained at a shear rate of 0.03 s^{-1}.

Visualization of the effect of solid loading

Scanning Electron Microscopy (SEM, Hitachi) imaging was used to visualize the effect of different solids loading (of 75 mass%, 76 mass% and 77 mass%) in the presence of constant amount 0.9 mass% of adsorbed Dolapix CE64 on stabilization of concentrated ZrO_2 nanosuspensions. In addition, SEM imaging used to visualize related packing quality and green microstructures that were prepared after drop casting of stabilized concentrated nanosuspensions and drying processes. An accelerating voltage of 15.0 kV applied for observation of dispersant coating quality on the surface structure of individual ZrO_2 nanoparticles. SEM samples were prepared by the suspension drop casting method with the use of SEM conductive carbon tape (Electron Microscopy Sciences, PA, USA). For each sample, a drop of freshly ball-milled suspension was taken and dripped manually onto the carbon tape and dried for 24h in air at room temperature.

Results and Discussion

Key parameters such as optimal viscosity, minimal amount of dispersant and high solids loading are beneficial for both mixing and casting in high concentrated slurry processing [51,52,56]. Some researchers have used zeta-potential studies, sedimentation, Capillary Suction Time (CST) measurements and viscosity measurements at fixed shear rates for low concentrated (e.g., < 60 mass% of solids loading) suspensions in assessing stability [1,46]. But for high concentrated systems, there exist insufficient reports and or studies.

It is, therefore, important to find out maximum solids loading and evaluate its effects on dispersion stability and rheological properties of ZrO_2 nanosuspensions [1,26,31]. Thus, to prepare highly stable slurry with optimal viscosity the maximum solid loading in suspensions was investigated by rheological measurements of ZrO_2 nanoparticle suspension batches. The solid loading concentration was varied from 75 to 78 mass% by measuring the suspension viscosity (η) and shear stress (τ), where the dispersant concentration in all suspensions was held at constant 0.9 mass%.

For rheological measurements, the first series of analyses were performed on suespensions containing of 78 mass% solids loading of ZrO_2 nanoparticles with a constant amount of 0.9 mass % dispersant. But this batch of nanosuspension exhibited a very strong shear-thinning behavior, paste structure, non-fluid and with high thixotropy which was not possible to apply for casting process. From this point of view, the experimental study centered on ZrO_2 nanoparticle suspensions of 75 mass % up to 77 mass % solids loading as a maximum possible solids loading. To evaluate rheological properties of each suspension composition, a rheological flow curve can be used. Flow curve can provide information that relates to the interactions among the nanoparticles, the polymer, and the aqueous

media. Furthermore, the strength of the interactions can be estimated with the information at various shear-rate conditions [37]. In particular, if the data can be represented by an appropriate rheological flow model, the evaluation may become more convenient and effective [38].Therefore, the results from rheological measurements are shown in figures 2A and 2B.

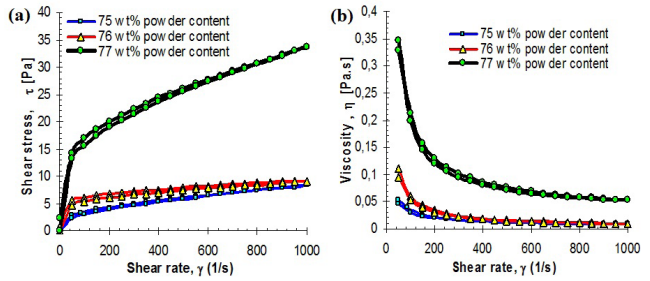

Figure 2: Rheological behavior of ZrO_2 nanoparticle suspensions with different solid loadings of 75 mass%, 76 mass% and 77 mass% with a constant amount 0.9 mass% of dispersant (Dolapix CE64); A) shows shear stress-versus-shear rate (flow curves), and B) shows dependence of viscosity on solid loading against shear rate.

Figures 2A and 2B, shows the variations in the rheological flow curves of shear stress τ (Pa) and viscosity η (Pa.s) as a function of shear rate γ < 0.03-1000 s^{-1}>) of concentrated ZrO_2 nanoparticle suspensions by different solid loadings with addition of a constant 0.9 mass% dispersant. Figures 2A and 2B, shows the loop lines of the shear stress and viscosity of the three suspensions with different solid loadings 75-77 mass% versus applied shear rates, γ ϵ < 0.03-1000 (s^{-1}) >. It is evident that all the three suspensions are characterised by "shear thinning" behavior [52-55].

Both the degree of shear thinning and the viscosity at high shear rates increase with increasing of solid loadings. This behaviour is common for all of concentrated, colloidally stable powder suspensions which are investigated in recent studies (also Al_2O_3 and ATZ suspensions) [3,36,41,56] and can be explained as a perturbation of the suspension structure by applied shear [57,58]. The thixotropy hysteresis was found and appeared more apparent when the solid loading of the suspension was over 75 mass%. On the other hand, figures 3A and 3B, shows the variations of shear stress and viscosity with respect to three different solid loadings for dispersion of ZrO_2 nanoparticle suspensions with constant addition (0.9 mass%) of Dolapix CE64 at three different shear rates of 50, 100 and 1000 s^{-1} at equivalent pH 9.0.

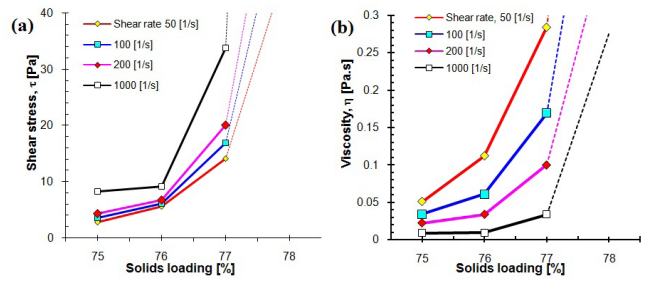

Figure 3 (A, B): The effect of solid loading on incremental increasing of shear stress τ (Pa) and viscosity η (Pa.s) of suspensions with constant amount (0.9 mass%) of dispersant (Dolapix CE64) at three different shear rates of 50, 100 and 1000 s^{-1}. (Equivalent pH); a) shear stress τ (Pa), and b) viscosity η (Pa.s) vs. solid concentration (mass%).

From figures 3A and 3B, it can be seen that,both shear stress and viscosity increase with solid loading which mainly attribute to the increase of hydrodynamic interaction between nanoparticles. That is to say, the viscosity of concentrated suspensions at a constant amount 0.9 mass% of dispersant depends strongly on solid loading, in this study.The viscosity at certain shear rate, γ 50 s^{-1}, with solids loading below 75 mass% shows minor changes and increases with the solids loading up to maximum 77 mass%. Keeping at shear rate as 50 s^{-1}, viscosity values of 0.05, 0.11 and 0.28 Pa.s were obtained with increasing solid concentration from 75, 76 to 77 mass%, respectively, see table 1.

Table 1 shows the relationship between solid loading (ϕ) and rheological properties such as viscosity, yield stress (τ_0) and relative variations in ZrO_2 nanoparticle suspensions by different flow models. A pronounced increase in τ_0 is apparently seen as maximum solids loading (ϕ_{max}) exceeds 77 mass% at a constant amount 0.9 mass% of dispersant. Table 1 also shows the experimental values of the shear-thinning (pseudoplastic) index (*n*), consistency coefficient (*k*) and yield stress (τ_0) of the above selected three suspensions with different solid loadings of 75, 76 and 77 mass%, which calculated automatically by fitting of their relative flow curves to the three different flow models of: power law [59], Herschel-Bulkley [59] and Bingham [60,61] from an extrapolation of the τ - γ (linear dependence) to $\gamma = 0$ s^{-1}. The value of (*n*) clearly demonstrates that all of the suspensions have shear thinning behaviour (*n* <1, *n* decreases) and exhibit a finite yield stress.

It is obvious that by increasing the solid loading of suspension, the viscosity, yield stress and thioxtropy of suspensions increases and also subsequenlty the fluid factor (*k*) drastically increases. This phonemenon is because of the larger number of interactions that any given particle has with its neighbors as ϕ is raised in the suspension system [62,63]. Finally, fitting the experimental data of table 1 by Herschel-Bulkley model, correlation coefficients of at least 0.998 are obtained indicating that the viscosity behavior of the examined suspensions can be described very well by the Herschel-Bulkley model.

As a supplementary step, to visualize the results obtained from rheological measurements, we test a hypothesis followed by a nanoscale schematic colloidal model. Our hypothesis is that at a constant amount (in this study: 0.9 mass% Dolapix CE64) of dispersant increasing of solid loadings from 75 mass% to 77 mass% not only influences on the rheological properties of concentrated ZrO_2 nanosuspensions, but also improves the packing structure of green bodies after casting. Accordingly, as solid loading increases in concentrated suspension it causes viscosity increasing. In addition, it helps green microstructures having better packing density that minimizes microstructure porosity. To visualize this hypothesis, a schematic nanoscale illustration of three types of colloidal models, using ZrO_2 nanoparticles as host particles and polyelectrolyte chains of dispersant Dolapix CE64 as the coating polymer, and mobile fluid as a background aqueous water, is shown in figures 4A-4C.

In addition, for further verification of our hypothesis in relation to each proposed colloidal model a scanning electron microscopy image of drop-cast sample after drying is included, see figure 4 (A, B, C). Our hypothesis focuseson the effect of solid loadings in the formation of high concentrated nanosuspensions with the relative lower viscosity (η < 0.2 Pa.s for shear rates above 100 s^{-1}, suitable for casting applications) at relatively constant pH value of 9.0, see figures 4A-4C. Figure 4A, shows a schematic illustration of our proposed model of

Sample (mass%)	Viscosity η (Pa.s)	Power law $\tau = k\gamma^n$			Herschel-Bulkley $\tau = \tau_0 + k\gamma^n$				Bingham $\tau = \tau_0 + \rho\gamma$			Thixotropy
(L= ϕ)	at γ = 50 (s^{-1})	k	n	r	τ_0	k	n	r	τ_0	ρ	r	Pa/s
75	0.05	0.44	0.42	0.999	0.06	0.45	0.43	0.999	2.56	0.006	0.99	215
76	0.11	1.60	0.39	0.999	0.10	2.73	0.42	0.998	4.97	0.005	0.80	474
77	0.28	2.60	0.37	0.999	0.75	2.79	0.17	0.998	13.52	0.020	0.92	567
78	Impossible	-	-	-	-	-	-	-	-	-	-	Paste

Table 1: The effect of solid loading on rheological properties (viscosity, yield stress and relative variations) of concentrated ZrO_2 nanosuspensions with constant amount 0.9 mass % of dispersant estimated by different flow models of: Power law, Herschel-Bulkley and Bingham models.

L: denotes the powder loading in mass %.

Note: The τ_0 represents the minimum stress needed to overcome before particles at rest are able to slide over adjacent particles in the liquid for the flow to occur.

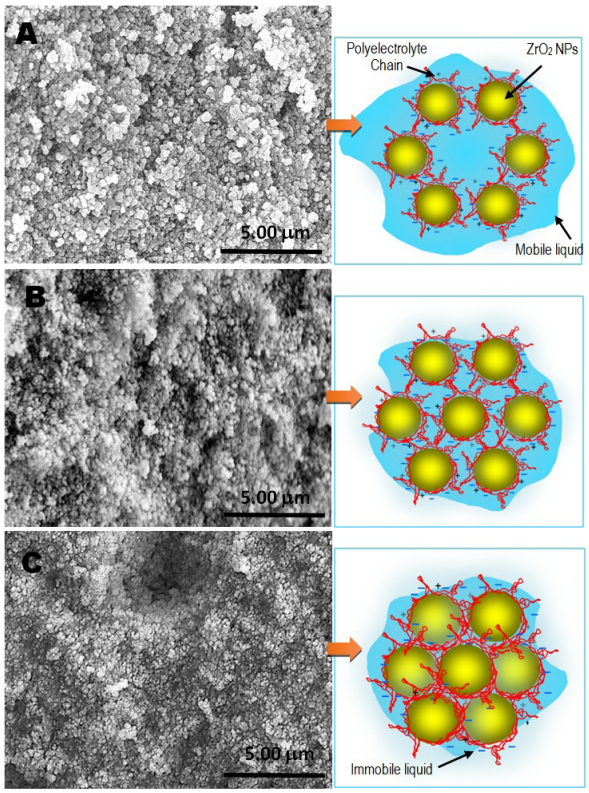

Figure 4 (A,B,C): Three schematic nanoscale colloidal models with related scanning electron microscopy images illustrating the effect of three different solid loadings of: A) 75 mass%, B) 76 mass%, and C) 77 mass% on colloidal packing and microstructure quality of samples prepared by concentrated ZrO_2 nanoparticle suspensions with a constant amount 0.9 mass% of anionic dispersant Dolapix CE64.

A: Sample with 75 mass% ZrO_2 NPs and open packing microstructure and extra mobile liquid area

B: Sample with 76 mass% ZrO_2 NPs and open packing microstructure and available mobile liquid area

C: Sample with 77 mass%ZrO_2 NPs and highly dense packing microstructure and immobile (less available) liquid area

colloidally dispersed ZrO_2 nanosuspension with constant 0.9 mass% dispersant and lower solid loading of 75 mass% ZrO_2 nanoparticles. As it can be seen, in this model dispersed nanoparticles have free colloidal space next to each other and there exists extra mobile aqueous liquid that can move among nanoparticles which helps lowering the viscosity. However, because of having lower solid loading and extra mobile liquid in this type of nanosuspension system it will cause aggregation among nanoparticles that increases larger pores and heterogeneity in green microstructure after casting. As it is evident from figure 4A, the SEM image shows large aggregation with pores among nanoparticles and hetegenuous microstructure.

However, figure 4B, shows a schematic illustration of our proposed second model for colloidally dispersed ZrO_2 nanosuspension with constant 0.9 mass% dispersant and higher solid loading of 76 mass% ZrO_2 nanoparticles. As it can be seen, in this model dispersed nanoparticles have less free colloidal space next to eachother and there exists available mobile aqueous liquid. Comparing to first model illustrated in figure 4A, in this model as its SEM image shows concentrated nanosuspension system has smaller aggregation among nanoparticles. But its mictrostructure still shows existing of heterogenuous packing formation which will lead to increasing viscosity and microstructure porosity that will negatively effect on the quality of final cast products.

In contrast to figures 4A and 4B, figure 4C shows a schematic illustration of third model of dispersed ZrO_2 nanosuspension with constant 0.9 mass% dispersant and maxmimum solid loading of 77 mass% ZrO_2 nanoparticles. As it can be seen, in this model dispersed nanoparticles have denser position next to eachother and there is not sufficient mobile liquid among them. In addition, the SEM image in figure 4C shows concentrated nanosuspension system which is denser and has much smaller aggregation and pores among nanoparticles with improved homogeneity in microstructure.

As a result, figure 4C demonstratesthe concentrated ZrO_2 nanosuspension that is dispsersed with constant 0.9 mass% dispersant and maxmimum solid loading of 77 mass% ZrO_2 nanoparticles has better rheological properties, green microstructure and packing quality, and therefore suitable for casting applications.

Conclusion

We have succcessfully prepared highly concentrated suspensions of biocompatible ZrO_2 nanoparticles with a constant amount of 0.9 mass% Dolapix CE64 which is a new type of an anionic polyelectrolyte dispersant, suitable for casting applications. The rheological properties of ZrO_2 nanoparticle suspensions including viscosity (η), shear rate (γ), and shear stress (τ) were investigated in relation to a wide range of solid loadings (ϕ, by weight = 75 - 78 mass%). The experimental results from the dependence of both viscosity and yield stress on solid loadings reveal that the maximum solid loading was estimated to be 77 mass%, which is suitable for casting of materials. For further validation, the maximum solid loading was compared and fitted by different rheological flow models with a correlation factor r = 0.998 for Herschel-Bulkley model, r = 0.999 for Power law model and r = 0.920 for Bingham model at shear rate γ (50 s^{-1}).

All concentrated ZrO_2 nanosuspensions exhibited shear-thinning behaviour. The results obtained from rheological measurements,

scanning electron miscroscopy imaging and flow models validate our proposed hypothesis for prediction of maximum solid loading and visualization of quality of green microstructures after casting.

Now, as we have gained the maximum solid loading of 77 mass% for concentrated ZrO_2 nanosuspensions with constant amount 0.9 mass% of dispersant, we suggest that for future work it is vital to further investigate the effects of different dispersant loadings on the stability and fluidity of concentrated nanosuspensions. This may result in maximum packing density, optimal viscosity, minimum porosity and defect-free microstructures in both green and sintered states after forming steps of final products.

Competing interests

The authors declare that they have no competing interests.

Authors' contributions

HS conceived the idea of formulating highly concentrated suspensions and using rheometry and high resolution electron microscopy techniques for characterization of concentrated nanoparticle suspensions, designed experimental protocols and setup development, involved in drafting the manuscript, participated in discussion, analyzed data, and coordinated the study. LS facilitated required funding and provided materials for experimental setup development, searched literature, coordinated the study, participated in discussion and involved in drafting the manuscript. LB and JH reviewed both theoretical and experimental protocols, made substantial contributions to conception and participated in discussion and data evaluation and analysis. VH prepared samples and led electron scanning microscopy experiments, interpreted and analyzed data, and participated in discussion. HA and AS participated in consultation, discussion, reviewing, data evaluation and overall results, and drafting the manuscript. All authors read and approved the final manuscript.

Acknowledgements

This work was accomplished through an international collaboration coordinated by H Sarraf. Authors are grateful to Prof. James K Beattie (School of Chemistry, University of Sydney, Australia) for his valuable comments, reviewing and technical advices related to colloidal dispersion of nanoparticles. Authors acknowledge Advanced Ceramics Department of TOSOH Corporation (Japan) and Tosoh Europe B.V. (Netherland) for collaboration, providing materials and partial research facilities. H Sarraf acknowledges the JSPS research associate fellowship awarded by Japan Society for the Promotion of Science and would like to thank Hori Katsuaki and Yuichi Suzuki, Center for Advanced Material Analysis, National Corporation Tokyo Institute of Technology, for their collaboration on high resolution-TEM analysis of nanoparticles.

References

1. Lange FF (1989) Powder processing science and technology for increased reliability. J Am Ceram Soc 72: 3-15.
2. Lewis JA (2000) Colloidal Processing of Ceramics. Journal of the American Ceramic Society 83: 2341-2359.
3. Sarraf H, Havrda J (2007) Rheological behavior of concentrated alumina suspension: Effect of electrosteric stabilization. Ceramics-Silikáty 51: 147-152.
4. Xu R (2008) Progress in nanoparticles characterization: Sizing and zeta potential measurement. Particuology. 6: 112-115.
5. Piconi C, Burger W, Richter HG, Cittadini A, Maccauro G, et al. (1998) Y-TZP ceramics for artificial joint replacements. Biomaterials 19: 1489-1494.
6. Chevalier J, De Aza AH, Fantozzi G, Schehl M, Torrecillas R (2000) Extending the lifetime of ceramic orthopaedic implants. Adv Mater 12: 1619-1621.
7. Heuer AH (1987) Transformation Toughening in ZrO_2-Containing Ceramics. Journal of the American Ceramic Society 70: 689-698.
8. Cao Y, Zhou YM, Shan Y, Ju HX, Xue XJ (2006) Triple-Helix Scaffolds of Grafted Collagen Reinforced by Al_2O_3-ZrO_2 Nanoparticles, Adv Mater 18: 1838-1841.
9. Piconi C, Maccauro G (1999) Zirconia as a ceramic biomaterial. Biomaterials 20: 1-25.
10. Bona AD, Pecho OE, Alessandretti R (2015) Zirconia as a Dental Biomaterial. Materials 8: 4978-4991.
11. Denrya I, Kelly JR (2008) State of the art of zirconia for dental applications. Dental Materials., 24: 299-307.
12. Mukherjee A, Maiti B, Sharma AD, Basu RN,Maiti HS (2001) Correlation between slurry rheology, green density and sintered density of tape cast yttria stabilized zirconia. Ceramics International, 27: 731-739.
13. Yoshikawa J, Lewis JA, Chun BW (2009), Comb Polymer Architecture, Ionic Strength, and Particle Size Effects on the $BaTiO_3$ Suspension Stability. Journal of the American Ceramic Society, 92: 42-49.
14. Sigmund WM, Bell NS, Bergström L (2000), Novel Powder-Processing Methods for Advanced Ceramics. Journal of the American Ceramic Society 83: 1557-1574.
15. Boaro M, Vohs JM, Gorte RJ (2003) Synthesis of Highly Porous Yttria-Stabilized Zirconia by Tape-Casting Methods. Journal of the American Ceramic Society 86: 395-400.
16. Hotza D, Greil P (1995) Review: Aqueous Tape Casting of Ceramic Powders. Materials Science and Engineering: A 202: 206-217.
17. Mironov V, Kasyanov V, Zheng Shu X, Eisenberg C, Eisenberg L (2005) Fabrication of tubular tissue constructs by centrifugal casting of cells suspended in an *in situ* crosslinkable hyaluronan-gelatin hydrogel.Biomaterials. 26: 7628-7635.
18. Zhang Y, Lu J, Yang S (2012) Preparation of hydroxyapatite ceramic through centrifugal casting process using ultra-fine spherical particles as precursor and its decomposition at high temperatures. Journal of Advanced Ceramics 1: 60-65.
19. Salomoni A, Tucci A, Esposito L, Stamenkovic I (1994) Forming and sintering of multiphase bioceramics. Journal of Materials Science: Materials in Medicine 9: 651-653.
20. Mallick KK (2009) Freeze Casting of Porous Bioactive Glass and Bioceramics. Journal of the American Ceramic Society 92: 85-94.
21. Vivanco J, Aiyangar A, Araneda A, Ploeg H-L (2012) Mechanical characterization of injection-molded macro porous bioceramic bone scaffolds. Journal of the Mechanical Behavior of Biomedical Materials 9: 137-152.
22. Aksakal B, Hanyaloglu C (2008) Bioceramic dip-coating on Ti-6Al-4V and 316L SS implant materials J Mater Sci Mater Med 19: 2097-2104.
23. Lewis JA (2006) Direct Ink Writing of Three-Dimensional Ceramic Structures. J Am Ceram Soc 89: 3599-3609.
24. Chang JC, Velamakanni BV, Lange FF, Pearson DS (1991) Centrifugal consolidation of Al_2O_3 and Al_2O_3/ZrO_2 composite slurries vs. interparticle potentials: Particle packing and mass segregation. J. Am. Ceram. Soc. 74: 2201-2204.
25. McCauley RA (1983) Ceramic Monographs. In: Handbook of Ceramics. Verlag Schmid GmbH, Freiburg, Germany, Pg No: 1-7.
26. H. Sarraf (2009) High performance ceramics by advanced colloidal processing. Appl Rheol 19: 2.

27. Sheppard LM (1991) The Changing Demand for Ceramic Additives. Am Ceram Soc Bull 69: 802-806.

28. Moreno R (1992) The role of slip additives in tape casting technology. Part 1: solvents and dispersants. Am Ceram Soc Bull 71: 1521-1531.

29. McHale AE (1991) Engineered Materials Handbook. Ceramics and Glasses, ASM International, Ohio, USA 4: 115-121.

30. Brinker CJ, Scherer GW (1990) Sol-Gel Science: The Physics and Chemistry of Sol-Gel Processing, Gulf Professional Publishing, Houston, USA.

31. Pugh RJ (1994) Surface and Colloid Chemistry in Advanced Ceramics Processing. In: Pugh RJ, Bergstrom L (eds.). Dekker M, New York, pp. 127-130.

32. Guo LC, Zhang Y, Uchida N, Uematsu K (1997) Influence of temperature of stability of aqueous Alumina slurry containing polyelectrolyte dispersant. Influence of temperature of stability of aqueous Alumina slurry containing polyelectrolyte dispersant 17: 345-350.

33. Okamoto H, Hashiba M, Nurishi Y, Hiramatsu K (1991) Fluidity and dispersion of alumina suspension at the limit of thickening by ammonium polyacrylates. Journal of Materials Science 26: 383-387.

34. Cesarano III J, Aksay IA (1988) Processing of highly concentrated aqueous α-Alumina suspensions stabilized with polyelectrolytes. J Am Ceram Soc 71: 1062-1067.

35. Foissy A, Attar AE, Lamarche JM (1983) Adsorption of polyacrylic acid on titanium dioxide. Journal of Colloid and Interface Science 96: 275-287.

36. Sarraf H, HerbigR, Maryška M (2008) Fine-grained Al_2O_3–ZrO_2 composites by optimization of the processing parameters. Scripta Materialia 59: 155-158.

37. Darby R (1986) Encyclopedia of Fluid Mechanics: Slurry flow technology. In: Cheremisinoff NP (ed.). Gulf Publishing Company, Houston, USA, pg no: 49-65.

38. Hiemenz PC, Rajagopalan R (1986) Principles of Colloid and Surface Chemistry. Marcel Dekker, New York, USA (a) pg no: 207-217, (b) ibid, pg no: 753-757, (c) ibid, pg no: 659-665.

39. Zhang F, Vanmeensel K, Inokoshi M, Batuk M, Hadermann J, et al. (2014) 3Y-TZP ceramics with improved hydrothermal degradation resistance and fracture toughness. Journal of the European Ceramic Society 34: 2453-2463.

40. Ozkurt Z, Kazazoğlu E (2010) Clinical success of zirconia in dental applications. J Prosthodont 19: 64-68.

41. Ban S (2008) Reliability and properties of core materials for all-ceramic dental restorations. Japanese Dental Science Review 44: 3-21.

42. Sarraf H, Herbig R (2008) Electrokineticsonic amplitude measurement of concentrated alumina suspension: Effect of electrosteric stabilization. Journal of the Ceramic Society of Japan 116: 928-934.

43. Tari G, Ferreira JMF, Fonseca AT, Lyckfeldt O (1998) Influence of particle size distribution on colloidal processing of alumina. Journal of the European Ceramic Society 18: 249-253.

44. Delgado AV, Gonzalez-Caballero F, Hunter RJ, Koopal LK, Lyklema J (2007) Measurement and interpretation of electrokinetic phenomena. Journal of Colloid and Interface Science 309: 194-224.

45. Gaydardzhiev S, Ay P (2006) Characterization of aqueous suspensions of fumed aluminium oxide in presence of two Dolapix dispersants. Journal of Materials Science 41: 5257-5262.

46. Rao SP, Tripathy SS, Raichur AM (2007) Dispersion studies of sub-micron zirconia using Dolapix CE64. Colloids and Surfaces A: Physicochemical and Engineering Aspects 302: 553-558.

47. Greenwood R (2003) Review of the measurement of zeta potentials in concentrated aqueous suspensions using electroacoustics. Advances in Colloid and Interface Science 106: 55-81.

48. Verhiest K, Mullens S, Wispelaere N de, Claessens S, DeBremaecker A, et al. (2012) Formulation and preparation of low-concentrated yttria colloidal dispersions. Ceramics International 38: 2701-2709.

49. Graule T, Hidber PC, Hofmann H, Gauckler LJ (1991) Stabilization of alumina dispersions with carboxylic acids. Proc. Euro-Ceramics II, Ausburg 1: 299-305.

50. Dakskobler A, Kosma [c-breve] T (2000), Weakly Flocculated Aqueous Alumina Suspensions Prepared by the Addition of Mg (II) Ions. Journal of the American Ceramic Society 83: 666-668.

51. Sarraf H, Qian Z, Skarpova L, Wang B, Herbig R, et al. (2015) Direct probing of dispersion quality of ZrO_2 nanoparticles coated by polyelectrolyte at different concentrated suspensions. Nanoscale Res Lett 10: 456.

52. Sarraf H, Sabet A, Herbig R, Havrda J, Hulínský V, et al. (2009) Advanced colloidal techniques for characterization of the effect of electrosteric dispersant on the colloidal stability of nanocrystalline ZrO_2 suspension. Journal of the Ceramic Society of Japan. 117: 302-307.

53. Mujumbar A, Beris AN, Metzner AB (.2002) Transient phenomena in thixotropic systems. Journal of Non-Newtonian Fluid Mechanics 102: 157-178.

54. Mewis J, Wagner NJ (2009) Thixotropy. Adv Colloid Interface Sci 147-148: 214-227.

55. Malkin AY, Kulichikhin VG (2015) Spatial-temporal Phenomena in the Flows of Multi-component Materials. Appl Rheol 25: 35358.

56. Liu X, Huang Y, Yang J (2002) Effect of rheological properties of the suspension on the mechanical strength of Al_2O_3-ZrO_2 composites prepared by gelcasting. Ceramics International 28: 159-164.

57. Xie Z, Ma JT, Xu Q, Huang Y, Cheng Y (2004) Effects of dispersants and soluble counter-ions on aqueous dispersibility of nano-sized zirconia powder. Ceramics International 30: 219-224.

58. de Kruif CG (1990) Hydrodynamics of disperse media. In: Hulin JP, Cazabat AM, Guyon E, Carmona F (eds.). Elsevier, North-Holland, Netherlands. Pg no: 79-101.

59. Herschel WH, Bulkley R (1926) Measurement of consistency as applied to rubber-benzene solutions. Proc Am Soc Testing Mater. 26: 621-633.

60. Ovarlez G, Barral Q, Coussot P (2010) Three-dimensional jamming and flows of soft glassy materials. Nature Materials 9: 115-119.

61. Jabbari M, Hattel JH (2014) Bingham plastic fluid flow model in tape casting of ceramics using two doctor blades-analytical approach. Materials Science and Technology 30: 283-288.

62. Carlstrom E (1994) Surface and Colloid Chemistry in Ceramics: An overview. In: Pugh RJ, Bergström L (eds.). Surface and Colloid Chemistry in advanced Ceramic Processing. Surfactant Science Series, Marcel Dekker Inc, New York, USA, 51: 1-28.

63. Russel WB, Saville DA, Schowalter WR (1989) Colloidal Dispersions. Cambridge University Press, Cambridge, UK.